Appendix A

ICET Background Information

List of Figures

List of Tables

This page intentionally left blank.

Appendix A. ICET Background Information

A.1. Project Test Plan Requirements

The ICET project represents a joint effort by the U.S. NRC and the nuclear utility industry, undertaken through the Memorandum of Understanding on Cooperative Nuclear Safety between the NRC and Electric Power Research Institute, Addendum on Integral Chemical Effects Testing for PWR ECCS Recirculation. As part of its contribution to the project, industry wrote "Test Plan: Characterization of Chemical and Corrosion Effects Potentially Occurring Inside a PWR Containment Following a LOCA." That test plan underwent several revisions during the ICET testing; Revision 12a was in place when ICET Test #1 began, and Revision 13 (Ref. A.1) was in place when Test #5 was conducted.

As stated in the test plan, the report addressed four topical areas: definition of test parameters, definition of the test loop, test performance, and characterization of test samples. The test plan served as the high-level guidance document for the ICET project. Selected information from the test plan is presented here.

The ICET project was begun with the objective of conducting five tests. Table A-1 shows the main parameters for each test. Each test ran for 30 days.

The materials included in the tests were zinc, aluminum, copper, carbon steel, concrete, and insulation materials such as fiberglass and cal-sil. The amounts of each material are given in the form of ratios (material surface area to water volume) in Table A-2, with three exceptions: concrete dust, which is presented as a ratio of mass to water volume, and fiberglass and cal-sil, which are presented as a ratio of insulation volume to water volume. Also shown in the table are the percentages of material that was submerged and unsubmerged in the test chamber.

Table A-1. Test Series Parameters

Run	Temp (°C)	TSP	NaOH	Sodium Tetraborate	pH	Boron (mg/L)	Notes
1	60	N/A	Yes	N/A	10	2800	100% fiberglass insulation test. High pH, NaOH concentration as required by pH
2	60	Yes	N/A	N/A	7	2800	100% fiberglass insulation test. Low pH, TSP concentration as required by pH.
3	60	Yes	N/A	N/A	7	2800	80% cal sil/20% fiberglass insulation test. Low pH, TSP concentration, as required by pH
4	60	N/A	Yes	N/A	10	2800	80% cal-sil/20% fiberglass insulation test. High pH, NaOH concentration, as required by pH.
5	60	N/A	N/A	Yes	8 to 8.5	2400	100% fiberglass insulation test. Intermediate pH, sodium tetraborate (borax) buffer.

Table A-2. Material Quantity/Sump Water Volume Ratios for ICET

Material	Value of Ratio for the Test (Ratio Units)	Percentage of Submerged Material (%)	Percentage of Unsubmerged Material (%)
Zinc in GS	8.0 (ft^2/ft^3)	5	95
Inorganic zinc primer coating (non–top coated)	4.6 (ft^2/ft^3)	4	96
IOZ primer coating (Top Coated)	0.0 (ft^2/ft^3)	–	–
Aluminum	3.5 (ft^2/ft^3)	5	95
Copper (including Cu-Ni alloys)	6.0 (ft^2/ft^3)	25	75
Carbon steel	0.15 (ft^2/ft^3)	34	66
Concrete (surface)	0.045 (ft^2/ft^3)	34	66
Concrete (particulate)	0.0014 (lbm/ft^3)	100	0
Insulation material (fiberglass or cal-sil)	0.137 (ft^3/ft^3)	75	25

The physical and chemical parameters that (1) are critical for defining the tank environment and (2) have a significant effect on sump-flow blockage potential and gel formation are summarized in Tables A-3 and A-4.

Table A-3. Physical Parameters for the ICET Tests

Water volume in the tank	949 L	250 gal.
Circulation flow	0–200 L/min	0–50 gpm
Spray flow	0–20 L/min	0–5 gpm
Sump temperature	60°C	140°F

Table A-4. Chemical Parameters for the ICET Tests

H_3BO_3 concentration	2800 mg/L as boron[a]
$Na_3PO_4 \cdot 12H_2O$ concentration	As required to reach pH 7 in the simulated sump fluid
NaOH concentration	As required to reach pH 10 in the simulated sump fluid
Sodium tetraborate (borax)	As required to reach boron concentration of 2400 mg/L
HCl concentration	100 mg/L*
LiOH concentration	0.7 mg/L as Li*

[a]Concentrations applicable for Tests #1 to #4. Concentrations for Test #5 are 2400 mg/L boron, 43 mg/L HCl, and 0.3 mg/L Li.

Appendix B contains information on ICET materials, including chemicals. Supplemental information is included here for concrete dust, latent debris, demineralized water, hydrochloric acid, sodium hydroxide, and lithium hydroxide.

Concrete dust was prepared by grinding material chipped from a corner of a surplus concrete coupon. Latent debris consisted of three size distributions and two different materials. Sand made up the two larger size distributions, which were 0.075–0.59 mm and 0.59–2 mm. These accounted for 35% and 28% of the total latent debris, respectively. Clay was used for the smallest size distribution, which was <0.075 mm.

Demineralized water was produced by reverse osmosis on-site using a commercially available Osmonics E-4 RO system, using tap water as the feed water, with no chemical additives. The conductivity produced by the system was typically <10 uS/cm (the test plan called for <50 uS/cm).

Hydrochloric acid was added as a liquid. It was ACS grade. The FW was 36.46 and assay (HCl) 36.5% to 38.0%. (Note: Actual concentrations of individual bottles were determined from lot numbers and used in calculations.) The source was EMD Corporation.

Sodium hydroxide was added as solid pellets. It was ACS grade. The FW was 40.00 and assay (NaOH) > 97%. The source was EMD Corporation.

Lithium hydroxide was added as anhydrous powder. The FW was 23.95 and the assay (LiOH) >96%. The source was Fisher Scientific Corporation.

Additional guidance in the test plan was translated into the ICET apparatus design, analytical methods and measurements of the test solution and samples, and project instructions within the QA program that determined test operations. Key aspects of these different areas are provided in Sections A.2 through A.4.

A.2. Test Apparatus Design

The functional design of the ICET test apparatus followed requirements in the test plan. Functional aspects of the test apparatus are as follows:

1. The central component of the system is a test tank. The test apparatus was designed to prevent solids from settling in the test piping.

2. The test tank can maintain both a liquid and a vapor environment, as would be expected in post-LOCA containment.

3. The test loop controls the liquid temperature at 60°C (±3°C).

4. The system circulates water at flow rates that simulate spray flow rates per unit area of containment cross section.

5. The test tank provides for submerged test coupons to be subjected to water flow that is representative of containment pool fluid velocities expected at plants.

6. Piping and related isolation valves are provided such that a section of piping can be isolated without interrupting the test.

7. The pump discharge line is split in two, one branch directing the spray header into the tank's vapor space and the other returning to the liquid side of the tank. Each branch is provided with an isolation valve, and the spray line includes a flow meter.

8. The recirculation piping includes a flow meter.

9. The pump circulation flow rate is controlled at the pump discharge to be within ±5% of the flow required to simulate fluid velocities in the tank. Flow is controlled manually.

10. The tank accommodates a rack of immersed sample coupons, including the potential reaction constituents identified in the test plan.

11. The tank also accommodates six racks of sample coupons that are exposed to a spray of liquid that simulates the chemistry of a containment spray system. Provision is made for these racks to be visually inspected.

12. The coupon racks provide sufficient space between the test coupons to preclude galvanic interactions among the coupons. The different metallic test coupons are also electrically isolated from each other and from the test stand to prevent galvanic effects resulting from metal-to-metal contact between specimens or between the test tank and the specimens.

13. The fluid volumes and sample surface areas are based on scaling considerations that relate the test conditions to actual plant conditions.

14. All components of the test loop are made of corrosion-resistant material (for example, SS for metallic components).

The as-built test loop consists of a test tank, a recirculation pump, 2 flow meters, 10 isolation valves, and pipes that connect the major components, as shown schematically in Figure A-1. P, T, and pH represent pressure, temperature, and pH probes, respectively. Figures A-2 and A-3 are photographs of the test loop and the data-acquisition system, respectively.

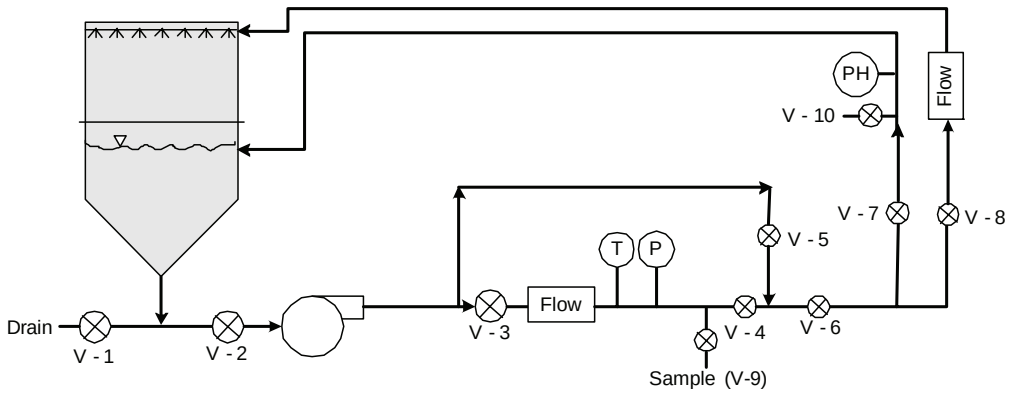

Figure A-1. Test loop process flow diagram.

Figure A-2. Photograph of the test loop.

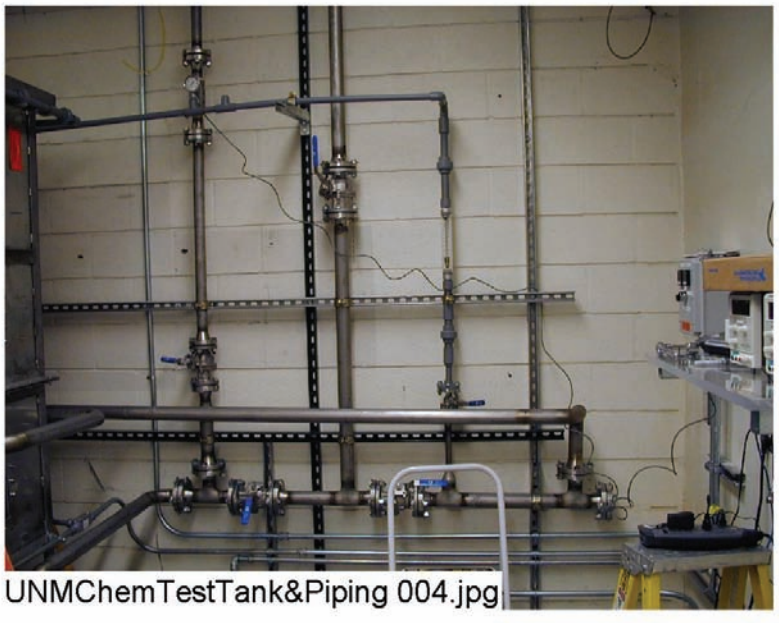

Figure A-3. Photograph of the data-acquisition system.

Materials

The tank, piping, and components were made of materials that are chemically resistant to a mixture of RO-treated water, sodium hydroxide, TSP, lithium hydroxide, hydrochloric acid, and boric acid in a pH range of 7.0 to 12.0 and a temperature of 140°F. Only one pH control chemical, either NaOH (resulting in a pH of ~10) or TSP (resulting in a pH of ~7), was used in a given test. The tank is constructed of type 304 SS, with polycarbonate view windows and Goretex® gaskets. The bottom portion of the tank is constructed of 1/8-in.-thick sheet steel, reinforced with 1/4-in.-thick by 2-in.-wide angle iron. The upper portion of the tank is constructed of 1/16-in.-thick sheet steel with 1/4-in.-thick by 2-in.-wide angle iron supports. The lid is 1/16-in.-thick sheet steel with 1/4-in.-thick by 2-in.-wide angle iron. One polycarbonate window with Goretex® gaskets is located in the bottom tank section, the top tank section, and the tank lid, for a total of three observation ports.

SS was used for the circulation piping to eliminate the possibility of chemicals leaching from the material into the solution. SS was also chosen for the recirculation pump, tank internals, and instruments to ensure that no leaching occurred. To facilitate the construction and assembly of the flow path from the recirculation piping to the spray nozzles, a different material, CPVC piping, was chosen.

Although leaching from the SS was not an issue, some of the other materials could not be guaranteed against leaching based only on their material descriptions. Thus, separate leaching tests were conducted with bench-scale experiments. CPVC pipe and the solvent used to connect fittings were soaked in a solution of the test chemicals for five days at 70°C. The solution was then tested; results indicated that the level of chloride (the element that might be expected to leach) was not detectable. A secondary concern was whether the CPVC would absorb chemicals, notably boron or sodium. The samples were tested, and results indicated only trace amounts of boron and sodium.

Similarly, the Goretex® gasket material was tested for possible leaching in the test solution chemistry. Chloride and silica are the two elements that could possibly leach from the gasket material. It was found that the scaled amount that did leach was 2 orders of magnitude less than what was expected from the test additives and fiberglass insulation.

Thus, it was concluded that the test apparatus materials would not contribute chemically to the test solution in concentrations that would impact the test results.

Tank Sizing

The tank holds 250 gal. of chemical solution, with 2–3 in. between the top of the water level and the top half of the tank. The bottom half of the tank can accommodate 250 gal. of solution, a single 60-coupon rack, and mesh cassettes containing 4 ft^3 of fiberglass insulation. The upper portion of the tank can accommodate 6 coupon racks, each containing up to 60 coupons. The tank is nominally 4 ft × 4 ft × 6.6 ft high, as shown in Figure A-4.

Figures A-4 through A-8 are photographs of the ICET tank, the cover lid, and the internal components, which include the top and bottom angle irons for supporting the racks, the distribution headers, the heaters, the thermocouples, and the spray nozzles.

Figure A-4. External view of the ICET tank.

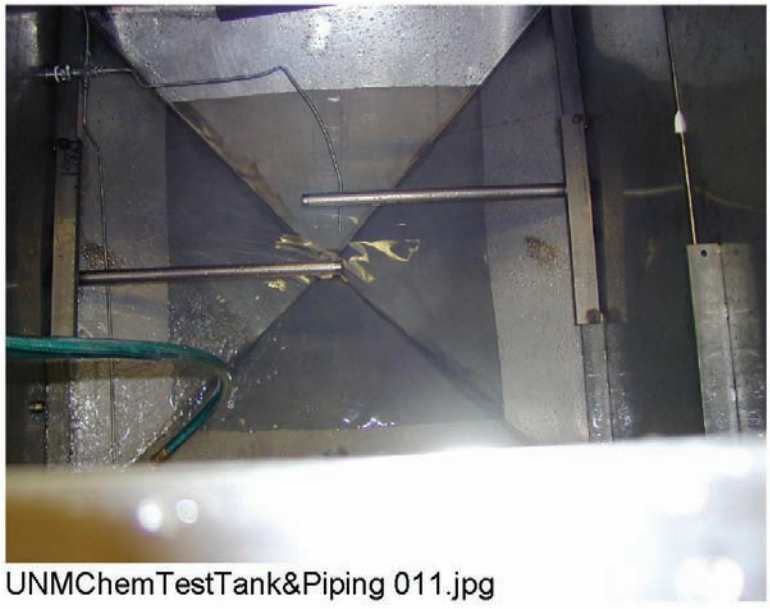

Figure A-5. The distribution header, heaters, and thermocouples inside the lower tapered reservoir of the ICET tank.

Figure A-6. The top and bottom angle irons for supporting coupon racks in the upper section of the ICET tank.

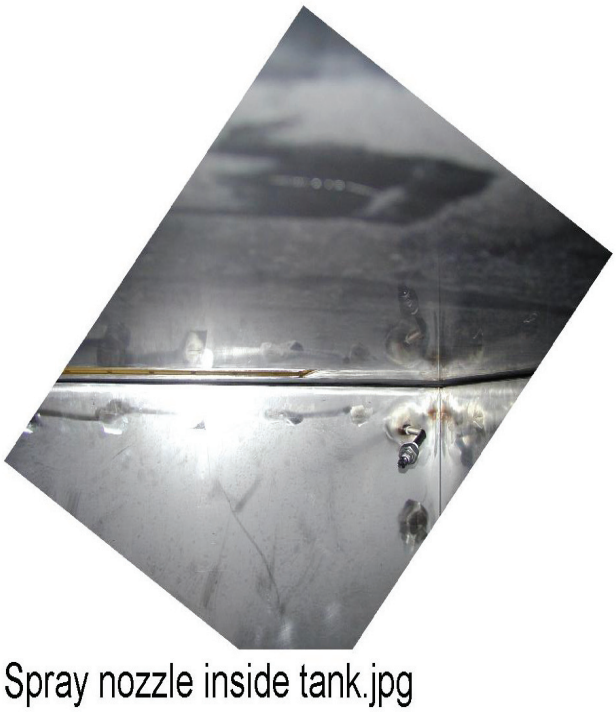

Figure A-7. One of four spray nozzles located in each upper corner of the ICET tank. This photo was taken through the upper access hatch while the lid was in place.

Figure A-8. The cover lid of the ICET tank showing the top observation window (lower) and top access hatch with handle (upper).

Figure A-9 and A-10 are as-built-dimensions drawings of the tank and piping system from both the front and side views, respectively. Given that the tank system is oriented approximately along the standard geographic compass directions, the front view depicts the east face of the tank, and the side view depicts the north face of the tank.

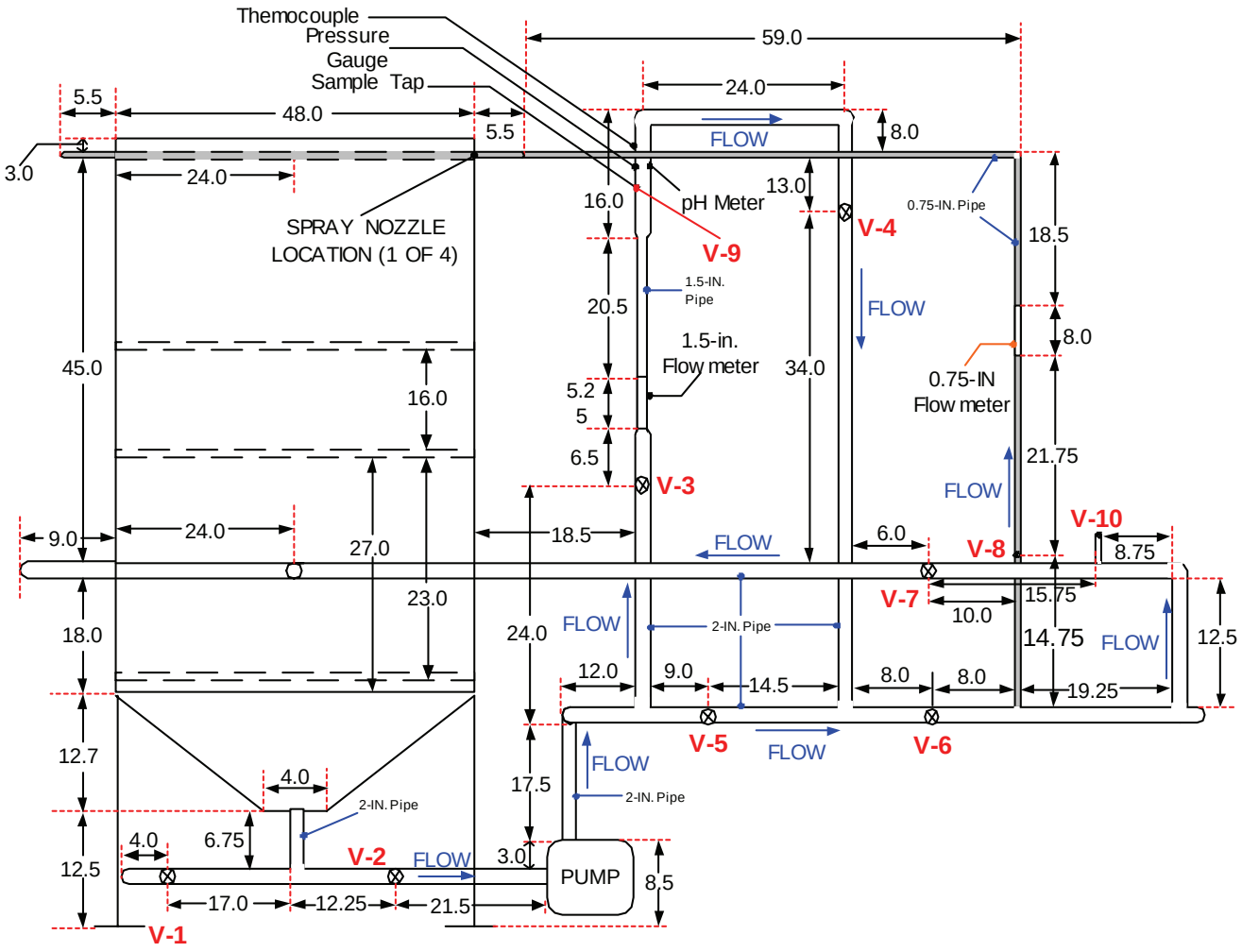

Figure A-9. Front-view, as-built dimensions of the tank and piping system. Dimensions are in inches; shaded regions represent CPVC piping.

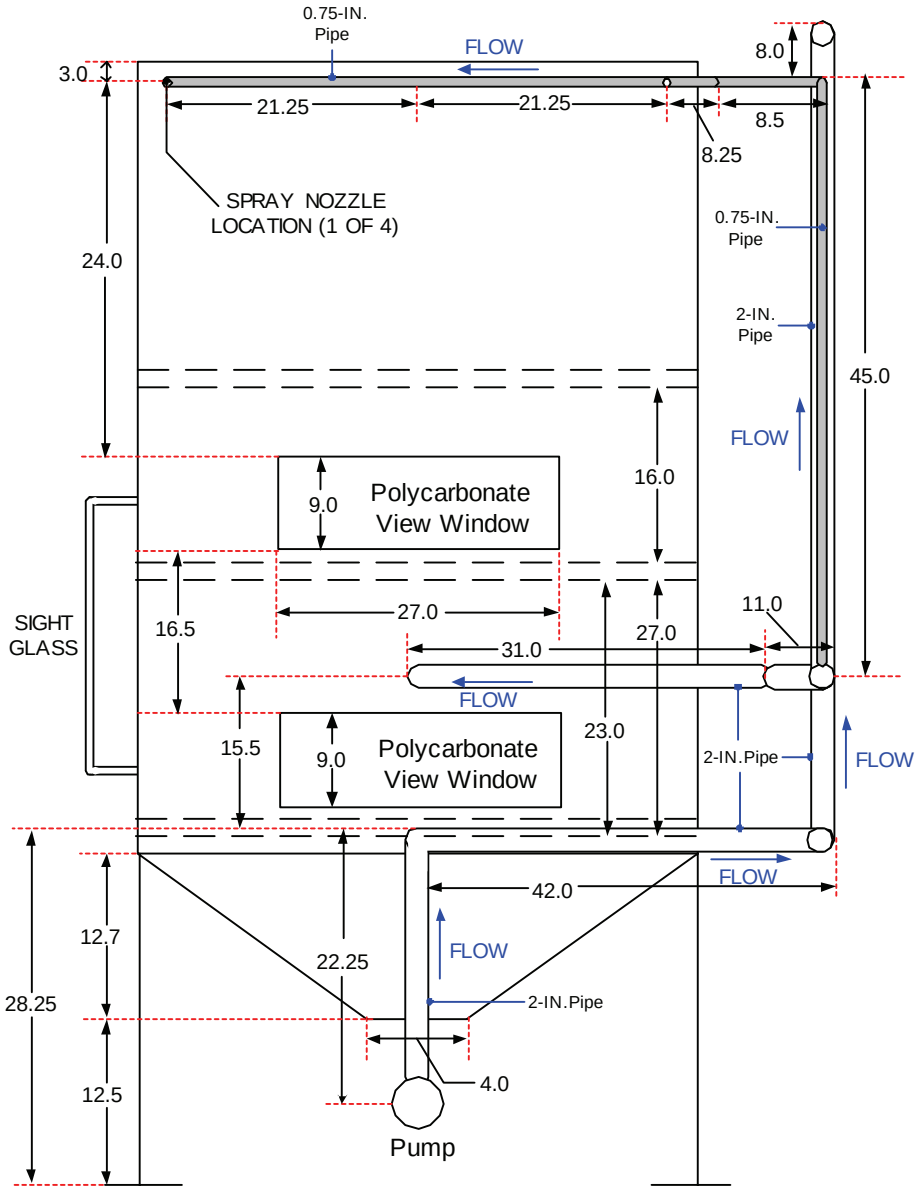

Figure A-10. Side-view, as-built dimensions of the tank and piping system. Dimensions are in inches; shaded regions represent CPVC piping.

Coupon Racks

The coupon racks are constructed of 1.5-in.-diam CPVC plastic piping. Figure A-11 shows a typical loaded rack. The racks prevent metal-to-metal contact between adjacent coupons and between the coupons and the rest of the tank assembly. This feature limits galvanic corrosion potential. Leaching tests were performed on the CPVC material and welding solvent to ensure that no detectable contributions to the chemical system would occur. Two complete sets of racks were built to facilitate staging of coupons for subsequent tests. The coupons can add up to 180 lb of weight to each CPVC-rack assembly. At elevated temperatures, the racks require support from 2-in.-wide SS angle irons strapped to the bottoms of the racks. These supports bridge the gap between the two sides of the tank and rest on the internal 2-in.-wide

SS angle irons. A 16-in. gap exists on each of the internal support angle irons to accommodate the lowering and emplacement of the nominal 14-in.-wide racks. The gap is then bridged with a length of angle iron that is pinned in place before the next tiers of racks are placed on top.

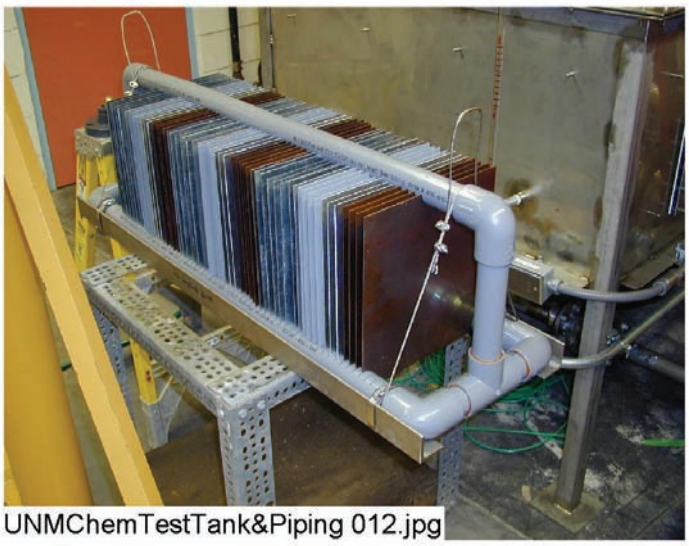

Figure A-11. Photograph of a loaded coupon rack.

Each ICET experiment exposed metallic and concrete coupons to anticipated post-LOCA environments. Each coupon is ~12 in. square. The metallic coupons are ~1/16 in. thick, except for the inorganic zinc-coated steel coupons, which are ~3/32 in. thick. The concrete coupons (one per test) are ~1-1/2 in. thick. Each test subjected seven racks of coupons to the specified environment, with one being submerged in the test tank and the remaining six being held in the tank's gas/vapor space. The number of each coupon type is shown in Table A-5.

Table A-5. Quantity of Each Coupon Type in Each Test

Material	No. of Coupons
Coated steel (CS)	77
Aluminum (Al)	59
Galvanized steel (GS)	134
Copper (Cu)	100
Uncoated steel (US)	3
Concrete	1

Note: Inorganic zinc (IOZ) coated steel and CS are the same coupon type.

The arrangement of the coupon racks in the test tank is schematically illustrated in Figure A-12. The figure shows a side view of the ICET tank, with the ends of the seven CPVC racks illustrated. The normal water level is indicated by the blue line in the figure. Rack 1 is the only submerged rack, and it sits on angle iron. It is centered in the tank so that flow from the two headers reaches it equally. Racks 2–4 are positioned above the water line, supported by angle iron in the tank. Racks 5–7 are positioned at a higher level, also supported

by angle iron. Racks 2–7 are exposed to spray. In the figure, north is to the right, and south is to the left. Directions are used only to identify such things as rack locations and sediment locations.

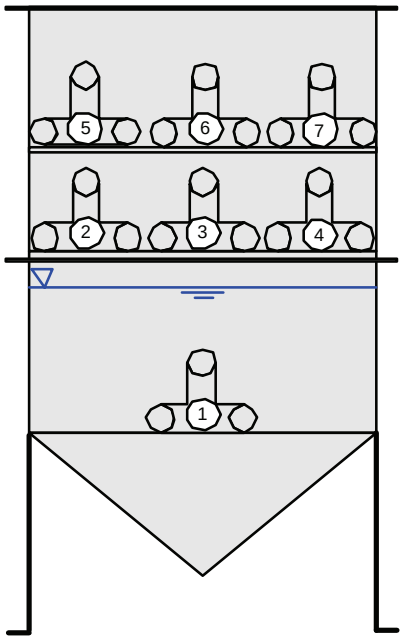

Figure A-12. Coupon rack configuration in the ICET tank. The blue line represents the surface of the test solution.

Figure A-13 shows the configuration of a typical unsubmerged coupon rack loaded with metal coupons and sitting in the ICET tank. The loading pattern of the racks was nearly identical, varying by only one or two coupons. Shown in the figure from left to right, the coupons are arranged as follows: four Cu, four Al, four inorganic zinc (IOZ), seven GS, four Cu, three Al, four IOZ, seven GS, four Cu, three Al, four IOZ, and seven GS.

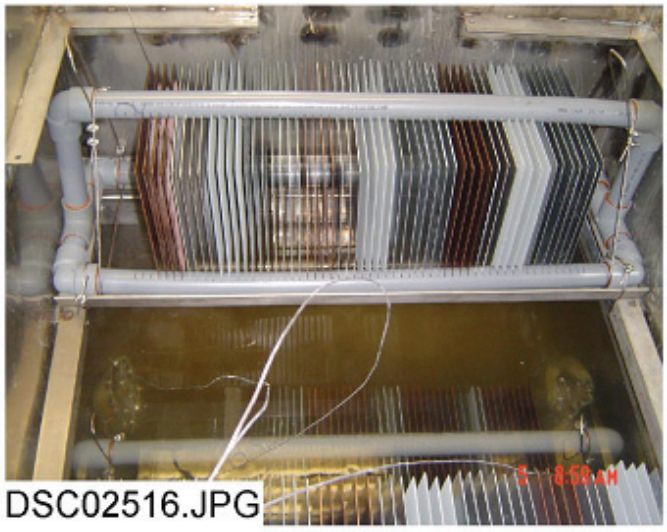

Figure A-13. A typical loaded coupon rack sitting in the ICET tank.

Tank Insulation

The tank is insulated with fiberglass boards. The surface area of the tank and top is ~130 ft^2. Approximately 50 linear feet of 2-in.-diam pipe remain uninsulated. The temperature of the fluid is nominally 140°F, and the outside surrounding air is ~70°F. The resulting heat loss from the tank and piping is ~1.2 kW.

Tank Heaters

The tank heaters are titanium jacketed to prevent corrosion and interaction of solution chemistry during the test series. Each heater is rated to supply 3.5 kW, thus providing excess (greater than the 1.2 kW required) redundant heating capacity and the ability to operate the tank assembly at higher temperatures if desired in the future. This additional capacity permits the convenience of having uninsulated piping runs. Under the existing electrical wiring configuration, only one heating element can be operated at a time. The locations of the two heaters inside the ICET tank are shown in Figure A-5.

Recirculation Pump.

The pump-wetted parts are SS, and the seals are compatible with boric acid and sodium hydroxide solutions. The pump is sized to provide a flow rate of up to 100 gpm. The pump has a variable speed controller so that the desired flow can be achieved, regardless of the system head loss. Loop shakedown resulted in a nominal flow rate of ~25 gpm during test operation. 25 gpm was chosen to yield fluid velocities over the submerged coupons from 0–3 cm/s. Figure A-14 is a photograph of the pump selected for the ICET system.

Figure A-14. Circulation pump for the ICET system.

Each of the two injection flow headers, placed below the water line along the top of the submerged coupon rack, consists of a 1-in.-diam pipe with a symmetric pattern of holes to distribute the solution discharge. The desired flow velocity across the submerged coupons was accounted for, along with the desired loop flow rate and pump characteristics. The

number and size of holes in the flow headers were calculated, and the holes were drilled symmetrically in each header. The primary goal of header design was to achieve a uniform flow pattern across the submerged coupons, with velocities in the 0–3 cm/s range. This velocity range is typical of that found in a post-LOCA containment pool. During loop shakedown activities, plastic streamers were placed at various spots in the tank to provide a visualization of the flow pattern. Then, the hole sizes were adjusted to achieve the desired pattern. Finally, food dye was introduced to determine the actual velocities. Tank velocities within the desired range were obtained.

The as-built configuration provided excess pressure head and flow capacity, even permitting for a doubling of the flow rate, if desired.

A.3 Analytical Methods and Measurements

Data collected during the ICET tests includes the on-line measurements of temperature, pH, and loop flow rate. During the water grab sample analysis, bench-top measurements were obtained for temperature, pH, turbidity, total suspended solids (TSS), and kinematic viscosity. Water, fiberglass, and metal samples are taken to other laboratory locations for additional analyses. These analyses include strain-rate viscosity, scanning electron microscopy (SEM), energy-dispersive spectroscopy (EDS), transmission electron microscopy (TEM), inductively coupled plasma (ICP) mass spectrometry, x-ray fluorescence (XRF), and x-ray diffraction (XRD). These analytical methods are described below.

Scanning Electron Microscopy (SEM)

The primary use of SEM is to study the surface topography of solid samples. The resolution of this technique is ~2 orders of magnitude better than optical microscopes and 1 order of magnitude less than TEM. SEM was used to examine the precipitate from the Day-15 and Day-30 high-volume water samples.

Principle of Operation. An electron beam passing through an evacuated column is focused by electromagnetic lenses onto the specimen surface. The beam is then scanned over the specimen in synchrony with the beam of the cathode-ray display screen. The incident beam electrons (from the electron gun) do not simply reflect off the sample surface. As the beam travels through the sample, it can do three things: First, it can pass through the sample without colliding with any of the sample atoms (matter is mostly space). Second, it can collide with electrons from the sample atoms, creating secondary electrons. Third, it can collide with the nucleus of the sample atom, creating a backscattered electron.

The incident beam is composed of highly energized electrons. If one of these electrons collides with a sample atom electron, an electron will be knocked out of its shell.

Figure A-15 illustrates this action. The released electron is called a secondary electron and is weak in energy. If these secondary electrons are close enough to the sample surface, they can be collected to form an SEM image.

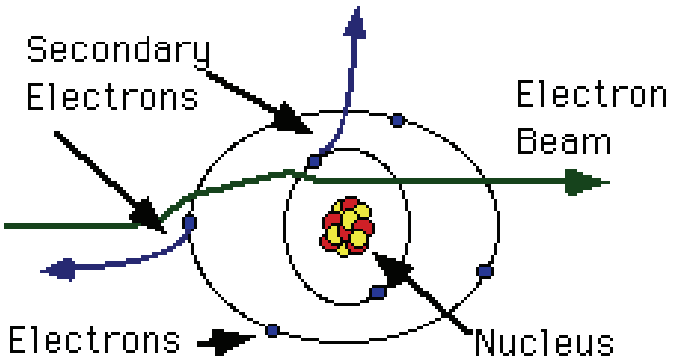

Figure A-15. Production of secondary electrons from an electron beam.

The incident beam electron loses little energy in this collision. In fact, a single electron from the beam will produce a shower of thousands of secondary electrons until it does not have the energy to knock these electrons from their shells. Inelastically scattered secondary electron emission from the sample is used to modulate the brightness of the cathode-ray display screen, thereby forming the image.

If the incident beam collides with a nucleus of a sample atom, it bounces back out of the sample as a backscattered electron (Figure A-16). These electrons have high energies, and because a sample with a higher density will create more of them, they are used to form backscattered electron images, which generally can discern the difference in sample densities. In this case, the image contrast is determined largely by compositional differences in the sample surface rather than by topographic features. Additional information on SEM may be found in Ref. A.2.

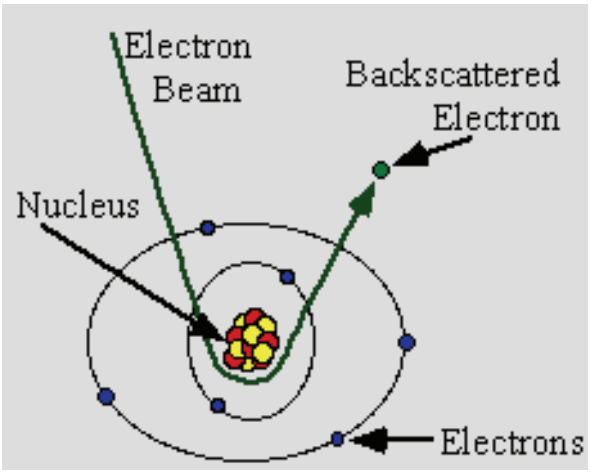

Figure A-16. Production of backscattered electrons from an electron beam.

Limitations. The principal limitation of SEM is the resolution. Typical resolution is limited to between 1.5 and 3 nm, which is ~1 order of magnitude less than TEM resolution. In addition, only the surface of the specimen can be viewed. Finally, the SEM operates under high vacuum and therefore is unsuitable for examining materials with a liquid component unless the materials dried first.

Energy-Dispersive Spectroscopy (EDS)

EDS can provide information on the elemental composition of a specimen. Combining the EDS system with SEM allows the microstructure-level identification of compositional gradients at grain boundaries, second phases, impurities, inclusions, and small amounts of material. EDS was used to examine the various structures formed on the fibers, which were similar for the Day-15 and Day-30 test samples. This examination allowed for a quantitative estimate of the elemental composition of the precipitate and the material deposited between the fibers.

Principle of Operation. As an incident electron beam interacts with the specimen, it loses energy. Characteristic x-rays are in turn emitted by the atomic species in the material. These characteristic x-rays are then converted into an electrical pulse with specific characteristics of amplitude and width. A multichannel analyzer measures the pulse and increments as a corresponding "energy slot" in a monitor display. The location of the slot is proportional to the energy of the x-ray photon entering the detector. The display is a histogram of the x-ray energy received by the detector, with individual "peaks," the heights of which are proportional to the amount of a particular element in the specimen being analyzed. Additional information on EDS may be found in Ref. A.2.

Limitations. The design of the equipment complicates the technique of detecting elements lighter than carbon. In general, a poorer sensitivity for light elements (low atomic weight) also exists in a heavy matrix. Resolution of the x-ray energy levels limits the positive identification of certain elements due to overlapping energy slots. Quantitative analysis is usually limited to flat, polished specimens. Unusual geometries, such as fracture surfaces, individual particles, and films on substrates can be analyzed, but with considerably greater uncertainty.

Transmission Electron Microscopy (TEM)

TEM is used to study the local structure, morphology, and chemistry of materials by examining the diffracted and transmitted electron intensities, as well as the characteristic x-rays and energies lost by the incident beam. TEMs are often coupled with EDS to give information about the local chemistry of the material. The high resolution of the TEM, at least 1 order of magnitude greater than SEM resolution, allows for qualitative size assessment of the underlying visible structures and aggregates. TEM was used on the precipitate from the Day-15 and Day-30 high-volume samples.

Principle of Operation. In transmission electron microscopes, a beam of high-energy electrons, typically 100–400 keV, is generated. The generated beam then is collimated by a magnetic lens and allowed to pass through the specimen under high vacuum. The resulting diffraction pattern, which consists of a transmitted beam and many diffracted beams, can be imaged on a fluorescent screen below the specimen. From the diffraction pattern, the lattice spacing information for the structure under consideration can be obtained. Alternatively, the transmitted beam or one of the diffracted beams can be used to form a magnified image of the sample. Finally, if the transmitted beam and one or more of the diffracted beams are

allowed to recombine, a high-resolution image can be obtained that contains information about the atomic structure of the material.

As the incident electron beam interacts with the specimen, it loses energy. Characteristic x-rays are in turn emitted by the atomic species in the material. These characteristic x-rays and the energy losses suffered by the incident electron can then be detected and analyzed to yield the EDS spectrum. Additional detail on TEM may be found in Ref. A.3.

Limitations. A TEM can have extremely high resolution, and research-level instruments can see individual atoms. However, a TEM has some limitations because the electron beam must travel through the sample, and lengthy sample preparation is usually required to make the sample thin enough. Because the beam is traveling though the sample, the sample bulk, not the surface, is being imaged.

Inductively Coupled Plasma - Atomic Emission Spectroscopy (ICP-AES)

ICP-AES is a rapid, sensitive way of measuring the elemental concentrations of solutions. More than 75 elements can be determined. ICP was used to determine the elemental composition of the daily water samples to assist in the overall understanding of the solution chemistry and corrosion behavior.

Principle of Operation. The first step in the procedure is conversion of the molecules in the sample to individual atoms and ions using a high-temperature, radio-frequency-induced argon plasma. The sample is introduced into the plasma as a solution. The sample is then pumped to a nebulizer, where it is converted to a fine spray and mixed with argon in a spray chamber. The purpose of the spray chamber is to ensure that only droplets in a narrow size range make it through into the plasma. Most of the sample drains away from the chamber; the rest is carried into the plasma and instantly excited by the high temperatures (5000–10,000 K). Atoms become ionized with 99% efficiency. The excited elements emit photons that are detected by one or more photomultiplier tubes. Additional information on ICP may be found in Ref. A.4.

Limitations. A notable limitation is the inability to measure hydrogen, carbon, nitrogen, and oxygen. In addition, silicon quantification is determined better by XRF because silicon will be lost to the vapor phase during ICP acid digestion procedures (as will certain trace elements, such as Hg, Se, As, and possibly Pb and Cd). The other notable disadvantage with the technique is that some minerals may not dissolve completely during the digestion procedure needed to use the ICP. Therefore, for samples containing substantial amounts of minerals (solids must be dissolved before analysis), XRF analysis is likely more appropriate for elemental determination. Interferences may also occur during ICP-AES due to overlap of the emission lines from the analyte and the interfering element and due to matrix effects. Finally, ICP is not suitable for determining chemical speciation.

X-Ray Fluorescence (XRF)

This x-ray technique is used to determine, both qualitatively and quantitatively, the elemental composition of a wide range of materials. XRF was used to examine the high-volume water sample precipitate on Days 15 and 30.

Principle of Operation. XRF is based on the photoelectric effect. When an atom is irradiated with highly energetic photons, an electron from one of the inner shells may be ejected (Figure A-17). As the vacancy is filled by an electron from an outer shell, a photon is released, the energy of which is characteristic of the atom. This radiation is called fluorescent radiation, and each element has its own set of characteristic emission lines. The intensity and the energy of these lines are measured using a spectrometer that detects wavelength-dispersive XRF or energy-dispersive XRF. Additional detail on XRF may be found in Ref. A.5.

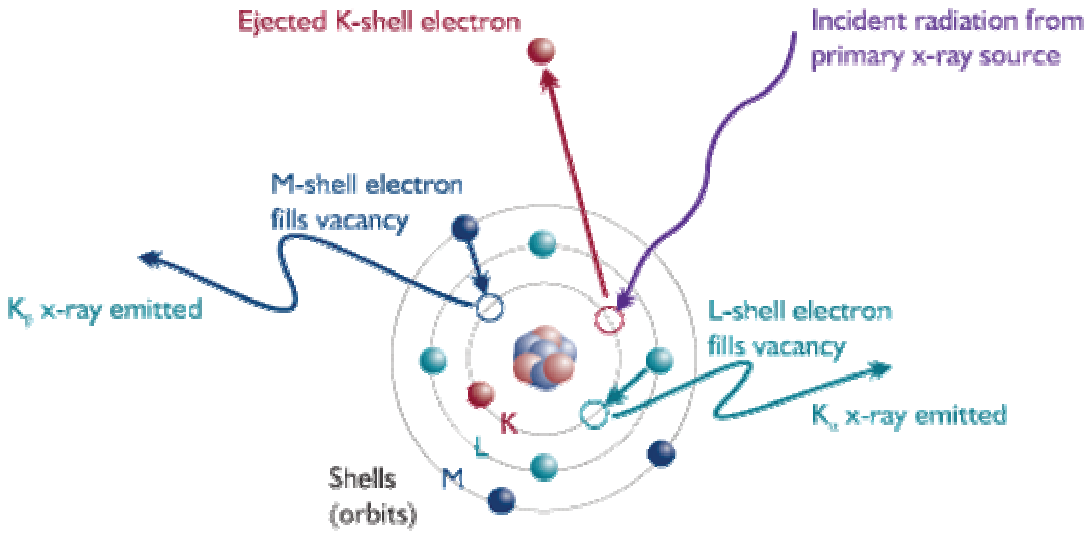

Figure A-17. Illustration of the operation principle of XRF.

Limitations. The accuracy of the results depends on how closely the standards resemble the sample. In addition, the principal limitation with this technique is the decreased sensitivity that occurs with decreasing atomic weight. Most XRF instruments cannot reliably detect elements lighter than carbon. Another limitation is that for accurate quantitative analysis, standards that are similar in composition and morphology to the unknown are required.

X-Ray Diffraction (XRD)

X-ray powder diffraction is used to obtain information about the structure, composition, and state of polycrystalline materials. The determination of the crystalline structure of the precipitate allows for the development of an understanding of the means by which the precipitate is formed. XRD analyses were performed on the post-test sludge precipitate. The target anode was copper in the x-ray tube.

Principle of Operation. If a beam of monochromatic x-rays is directed at a crystalline material, reflection or diffraction of the x-rays is observed at various angles with respect to the primary beam. The relationship between the wavelength of the x-ray beam, λ, the angle of diffraction, 2θ, and the distance between each set of atomic planes of the crystal lattice, d, is given by the Bragg equation:

$$N\lambda = 2\,d\sin\theta \ ,$$

where N represents the order of diffraction.

From this equation can be calculated the interplanar distances of the crystalline material being studied. The interplanar spacing depends solely on the dimension of the crystal's unit cell, whereas the intensities of the diffracted rays are a function of the placement of the atoms in the unit cell.

Limitations. Conventionally, the largest limitation of XRD is its restriction to crystalline materials because amorphous materials do not diffract. Milligram samples may be analyzed if the analysis time is not important. The requirement of sample quantity (typically several hundred milligrams) is to provide the enormous number of small crystallites oriented in every conceivable direction. Thus, when an x-ray beam traverses the material, a significant number of the particles can be expected to be oriented to fulfill the Bragg condition for reflection from every conceivable interplanar spacing.

Wet Chemistry Analyses

The standard methods used for wet chemistry analyses are shown in Table A-6. Additionally, the following paragraphs provide supplemental data for nonstandard methods.

Table A-6. Methods for Wet Chemistry Analysis

Parameter	Method[a]	Major Equipment
pH	SM 4500-H^+ (Electrometeric)	Orion Model 720 A
Turbidity	SM 2130 (Nephelometeric)	Hach Turbidimeter Model 18900
Total suspended solids	SM 2540D	–
Temperature	SM 2550	–
Kinematic viscosity	–	Cannon-Fenske Capillary Viscometer
Shear-rate viscosity	-	Bohlin CS-10 rheometer

[a]SM = *Standard Methods for the Examination of Water and Wastewater* (20th Edition) (APHA et al. 1998).

The pH meter was calibrated before use with a three-point calibration curve using certified pH buffers at 4, 7, and 10. The pH was recorded to the nearest 0.01 pH unit. The bench-top pH measurements correspond to the actual temperature of the sample at the time it was measured. An automatic temperature compensation pH probe was used to provide a temperature-corrected pH, using a 3-point calibration curve. It is noted that pH varies by only 0.04 units between 25ºC and 60ºC within the pH range of interest. So, the temperature had very little effect on the measurements that were reported. The turbidimeter was calibrated with Gelex secondary standards before testing. Turbidity was recorded to the nearest 0.01 Nephelometric Turbidity Unit (NTU).

For TSS, a standard volume of 500 mL was filtered for all samples. A 0.7-µm glass fiber filter was used. The filters were weighed in aluminum boats for the pre-sample and post-sample weights, with the post-sample filters completely dried in an oven. The difference in weights was the amount of TSS in the volume, and the TSS was recorded to the nearest 0.1 mg/L.

Kinematic viscosity was measured with a Cannon-Fenske capillary viscometer, size 50. Viscosity was measured on both filtered and unfiltered samples, each at a temperature of 60(±1.0)°C [140(±1.8)°F] and again at 23(±2.0)°C [73.4(±3.6)°F]. The viscosity of water is highly sensitive to temperature, and the allowed temperature range results in a variation of viscosity of 2% between 59°C (138.2°F) and 61°C (141.8°F) and a 9.3% variation between 21°C (69.8°F) and 25°C (77.0°F). For this reason, temperature was measured to 0.1°C accuracy with a National-Institute-of-Standards-and-Technology-traceable thermometer for all viscosity measurements, and the measured viscosity values were corrected to a common temperature to facilitate comparisons. The corrected temperatures chosen for comparison were 60.0°C (140°F) and 23.0°C (73.4°F). Equations were derived to correct viscosity by fitting an equation to viscosity data and minimizing the coefficient of determination (R^2). The formulas used to correct the viscosity were

$$\nu_{23} = \nu_M \left(1.0235\right)^{(T_M - 23)}$$

and

$$\nu_{60} = \nu_M \left(1.0146\right)^{(T_M - 60)} \quad ,$$

where

T_M = temperature at which viscosity measurements are made (°C),
ν_M = measured kinematic viscosity at temperature T_M (mm^2/s),
ν_{60} = kinematic viscosity corrected to 60.0°C (mm^2/s), and
ν_{23} = kinematic viscosity corrected to 23.0°C (mm^2/s).

In addition, duplicate measurements were made at each condition until Day 25 of the test. In nearly all cases, the replicate viscosity measurements varied by considerably less than 1%. From Day 25 of Test #1, duplicate measurements of viscosity were no longer taken because of the consistency previously noted.

Shear-rate viscosity was measured using a Bohlin CS-10 rheometer. The instrument was calibrated, and a trained operator followed the manufacturer's instructions to obtain the actual measurements. Samples were analyzed after 1 day of testing and weekly thereafter. Both filtered and unfiltered samples were analyzed for Test #1. Because there were no significant differences between filtered and unfiltered, only unfiltered samples were analyzed for Tests #2 through #5.

All measurements were conducted with a shear-stress range of 0.0095 to 0.12 Pa. Samples were first measured at 60ºC and then cooled to 25ºC. The samples were transported to the Bohlin CS10 Rheometer in a cooler containing a hot-water bottle to maintain a warm temperature. Any samples that were not immediately analyzed were placed into an oven set at 60ºC until they could be measured. When samples were placed in the rheometer, their temperatures were controlled to the desired value. Through this procedure, the test sample was maintained continuously at the desired temperature.

The purpose of shear-rate viscosity measurements was to investigate the physical response of the test solution to a driving shear-stress. The conclusion derived was whether the solution behaved as a Newtonian or non-Newtonian fluid.

A.4 QA Program

A project QA manual was developed to satisfy the contractual requirements that applied to the ICET project. Specifically, those requirements were to provide credible results by maintaining an appropriate level of QA in the areas of test loop design, sampling, chemicals, operation, and analysis. These requirements were summarized in the contract requirement that QA was to be consistent with the intent of the appropriate sections of 10CFR50, Appendix B.

The 18 criteria of 10CFR50, Appendix B, were addressed separately in the QA manual, and the extents to which they apply to the ICET project were delineated. A resultant set of QA procedures was developed. In addition, test-specific project instructions (PIs) were written to address specific operational topics that required detailed step-by-step guidance. PIs generally applicable to all tests were written for the following topics:

- Data Acquisition System (DAS)
- Coupon Receipt, Preparation, Inspection, and Storage
- DAS Alarm Response
- Chemical Sampling and Analysis
- TEM Examination of Test Samples
- SEM Characterization of Test Samples
- Viscosity Measurements

Each project instruction that governed test operations was revised for nearly every test. Those PIs consisted of the following:

- Pre-Test Operations
- Test Operations
- Post-Test Operations

Beginning with the Test #2 data report, the test-specific PIs for pre-test, test, and post-test operations were included as report appendices.

Samples from the tests were taken to an off-site analytical laboratory for ICP-AES analyses. That laboratory operated according to its own approved QC program. To ensure the accuracy of the ICP results, several QC steps were performed with every batch of samples run on the instrument. Those QC steps were as follows:

Lab Control Spike (LCS)—The LCS consists of a known concentration of each analyte (typically 1 to 5 mg/L, depending on analyte) in deionized water. The measured concentration is compared with the spike concentration, and a percent recovery is reported. An exception is noted if the percent recovery of any analyte is outside the acceptable range. The acceptable range is based on previous QA procedures developed for the instrument.

Method Blank (MB)—The MB is a sample of deionized water. All analytes are expected to be below the detection limit. An exception is noted if the measured concentration of any analyte is above the detection limit.

Matrix Duplicate (MD)—The MD is a second analysis of one of the samples in the run. The measured concentration for each analyte is compared between the two samples, and an exception is noted if the two results do not agree to within 20%.

Matrix Spike (MS)—The MS consists of a known concentration of each analyte (typically 1 to 5 mg/L, depending on analyte) added to one of the samples in the run. The difference in the measured concentrations between the original sample and spiked sample is compared with the spike concentration, and a percent recovery of the spiked concentration is reported. An exception is noted if the percent recovery of any analyte spike is outside the acceptable range.

Matrix Spike Duplicate Accuracy (MSDA)—The MSDA is a repetition of the MS. An exception on the MSDA is identical to an exception on the MS.

Matrix Spike Duplicate Precision—The two runs of the matrix spikes (MS and MSDA) are compared with each other. An exception is noted if the two measured spike concentrations do not agree to within a relative percent difference of 20%.

Serial Dilution—One of the samples in the run is diluted with deionized water by a factor of 5. The measured concentration of the diluted sample is compared with the predicted concentration, which is calculated from the dilution rate and the measured concentration of the original (undiluted) sample. An exception is noted if the differences between the measured and calculated concentrations are not within the acceptable range.

It was necessary for the analytical laboratory to perform a 10:1 dilution of the samples to lower the concentration of borate to reduce interferences between borate and the analytes. This process had the effect of raising the detection limit for these analyses to a value 10 times higher than the instrument detection limit, but the higher detection limit had no impact on the results. The instrument detection limit was significantly below 1 mg/L for all analytes, and the higher detection limit was still well below the levels of concern for this experiment.

The water samples were totally digested before the ICP measurement and represented the solution plus any precipitate present. Samples were kept at 4ºC after they were extracted until they were digested. Each laboratory batch of samples had its own specific uncertainty, depending on the results of its QC checks. They were within the accepted uncertainties of the laboratory QC program, or the analyses were rerun. A typical set of measurement uncertainties was as follows: aluminum, ±20%; calcium, –14% and +19%; sodium, ±20%; magnesium, –13% and +20%; and silica, –9% and +12%. The minimum detection limits are given in Table A-7.

Table A-7. ICP-AES Minimum Detection Limits for Elements, in mg/L

Cl	B	Ca	Pb	Li	Mg	K	Si	Zn	Na	Al	Cu	Fe	Ni
0.5	0.01	0.5	0.005	0.002	0.5	0.5	0.5	0.01	1.0	0.05	0.02	0.01	0.002

A.4. References

A.1. "Test Plan: Characterization of Chemical and Corrosion Effects Potentially Occurring inside a PWR Containment Following a LOCA, Rev. 13," July 20, 2005.

A.2. Goldstein, J., Scanning Electron Microscopy and X-ray Microanalysis, 2nd ed., Plenum Press: New York (1992).

A.3. Williams, D. B., "X-ray Spectrometry in Electron Beam Instruments; Plenum Press: New York (1995).

A.4. Montaser, A., "Inductively Coupled Plasmas in Analytical Atomic Spectrometry"; VCH Publishers, Inc.: New York (1987).

A.5. Jenkins, R., "Quantitative X-Ray Spectrometry, Marcel Dekker Inc.: New York (1981).

This page intentionally left blank.